Kinetics of methylene blue degradation in VUV/UVC irradiation process and the role of hydroxyl radical

Cong Geng (gengcong-7.16@163.com)
Shenyang University of Technology https://orcid.org/0000-0002-2277-8126
Jialiang Liang
Chongqing University
Zhijie Liang
Chongqing University
Zhiwei Zhao
Chongqing University
Yinyan Guan
Shenyang University of Technology
Weichun Gao
Shenyang University of Technology
Jiyan Liang
Shenyang University of Technology

Research Article

Keywords: Vacuum UV, Chemical-free, Methylene blue, Degradation mechanism, Hydroxyl radical

Posted Date: April 21st, 2022

DOI: https://doi.org/10.21203/rs.3.rs-1349045/v1

Abstract

A series of investigations have been carried out to study the decomposition of methylene blue (MB) by the VUV/UVC based AOPs. However, MB degradation by VUV/UVC direct photolysis has not been reported previously. For the first time, the degradation kinetics and mechanisms of methylene blue by a chemical-free technology VUV/UVC (185 nm/254 nm) irradiation were systematically investigated in bench scale. Firstly, we investigated the impact of reaction conditions (i.e., VUV power, temperature, initial pH, and initial MB concentration on the VUV/UVC irradiation process. We found that MB degradation by VUV/UVC irradiation is an endothermic reaction, and the apparent activation energy was calculated to be 14.72 $kJ{\cdot}mol^{-1}$, which is similar UVC/TiO_2 and electrical discharge plasma system, while higher VUV power and lower initial MB concentration have enhancement effects. The degradation rate constant was a convex function of the solution pH and reached the optimal value at pH 9.19. Compared with VUV/UVC irradiation and UVC/H_2O_2 processes, hydroxyl radical (·OH) plays the dominated role in VUV/UVC irradiation system, while both ·OH and HO_2· contribute to conventional UVC/H_2O_2 process. The degradation pathways were proposed including demethylation and chromophores oxidation, and the possible pathway was confirmed by combining the experimental observations with the density functional theory (DFT) calculation. In summary, this study provides the results that VUV/UVC is an effective and chemical-free technology for MB removal from water.

1. Introduction

Organic dyes are extensively usage in food processing, paint (Islam et al. 2020), printing (Kecić et al. 2018), textile industries (Badmus et al. 2020) and leather tanning (Xu et al. 2020), etc. Unfortunately, a large quantity of organic dyes wastewater produced during its producing and consuming (Hasanpour &Hatami 2020) and caused serious problems to human health, aquatics and plants (Berradi et al. 2019). Moreover, the presence of organic dyes in industrial effluent has become one of the major challenge of wastewater treatment (Mittal et al. 2018, Tkaczyk et al. 2020). Organic dyes wastewater is difficult to treat satisfactorily using conventional wastewater treatment process due to its complex composition, deep color, strong toxicity, large water quantity, stable nature and high organic content (Singh &Arora 2011). Over the past few decades, hydroxyl radical (·OH)-based advanced oxidation processes (AOPs) are considered as an effective and promising method for the degradation and mineralization of the organic contaminants in wastewaters. A number of AOPs methods have been development to produce ·OH such as UV/H_2O_2 (Zhang et al. 2019a), Fenton (Zárate-Guzmán et al. 2019), ozonation (Wang et al. 2019) electrochemical oxidation (Liang et al. 2015) and photocatalysis (Lin et al. 2016). However, these AOPs process need adding external chemical as oxidant, catalyst, electrolyte, etc., which need a consistent chemical supply (Krichevskaya et al. 2011). Therefore, development of an efficient and chemical-free technology for organic dyes wastewater is always in need.

Recent years, a novel chemical-free AOP that set Vacuum UV (VUV) as the light source has gained increasing attention. VUV AOP was found to be an efficient and economical method compared with

traditional UV-based AOPs by effective utilization of the in situ generated reactive oxygen species (Zhang et al. 2021). VUV is a form of electromagnetic radiation with wavelength from 100 nm to 200 nm which corresponds to high photon energy (Zoschke et al. 2014). Under the VUV radiation, ·OH, hydrogen atoms (·H), and solvated electrons (e_{aq}^-) are generated by the photochemical ionization of water molecule (Eqs. 1 and 2).

$$H_2O \xrightarrow{\lambda=185nm} \cdot OH + H^+ + e_{aq}^- \quad (1)$$

Φ(e_{aq}^-) = 0.045 [21]

$$H_2O \xrightarrow{\lambda=185nm} \cdot OH + H \cdot \quad (2)$$

Φ(·OH) = 0.33 [21]

Low pressure mercury lamps (LPUV) is a kind of typical VUV light source which using synthetic silica in the production of the lamp tube (Li et al. 2016). LPUV (known as VUV/UVC) illuminate a limited number of well-defined lines, which concentrate at 253.7 nm (UVC, nominal value: 254 nm) and 184.9 nm (VUV, nominal value: 185 nm) (Zoschke et al. 2014). VUV/UVC are mostly used as VUV light source for eliminating organic pollutants from water. In previous studies, microcystin-LR (Chintalapati &Mohseni 2020), carbamazepine (Zhu et al. 2019), imipramine (Xie et al. 2019), tris(2-chloroethyl) phosphate (Chen et al. 2019) and fluoroquinolone antibiotics (Geng et al. 2020) have been proved to be efficiently removed in VUV/UVC irradiation process. Because of high efficacy and cost-effective, VUV/UV irradiation process is a promising technique for the treatment of waters contaminated with organic pollutants (Moussavi &Shekoohiyan 2016). A series of previous studies have investigated the degradation of methylene blue by VUV/UVC based AOPs, such as VUV/UVC/TiO_2 (Huang et al. 2013), VUV/UVC-photo-Fenton (Li et al. 2016) and VUV/UVC/persulfate (Wen et al. 2020) process. However, the mechanism and kinetics of methylene blue degradation in VUV/UVC direct irradiation process have been no reported so far, and many questions remain to be investigated.

In this study, MB was selected as a target organic dye for investigating the degradation kinetics and mechanisms in VUV/UVC irradiation process. The evaluation of MB degradation efficiency was employed in UVC alone, VUV/UVC alone and UVC/H_2O_2 process. Active oxygen species (ROS) quenching tests and UV-Vis spectrum characterization were used to confirm the degradation mechanism. The effect of important operational factors, including VUV power, temperature, initial solution pH, and initial MB concentration were evaluated on the performance of MB degradation in VUV/UVC process. The major organic and inorganic byproducts were identified, and the degradation pathway of MB was proposed.

2. Material And Method

2.1. Chemicals

Methylene blue, potash iodide, and ammonium molybdate were purchased from Chron Chemical, China. 1.4-benzoquinone, potassium acid phthalate, and sodium bicarbonate were purchased from Sinopharm Group Co., China. Chemicals used for experiments were reagent grade and without further purification. All solutions were prepared with ultrapure water produced from a Direct-Pure UP water purification system (RephiLe Bioscience, China).

2.2. Experimental procedures

The degradation experiments were conducted in a photo-reactor, shown in Fig. S1, and the description was in Text 2. All the batch experiments for MB degradation were performed in a lab scale annular photo-reactor. A glass column (50mm×250mm) with a working volume of 300 mL, and reaction temperature was adjusted and kept with a thermostatic water bath (THD-1015, Ningbo Tianheng, China). An 8 W low pressure mercury lamp (Beijing Aerospace Hong Da Optoelectronics Technology Co., China) was the experimental light source, which could emit VUV/UVC (10-08100, emitting at both 185 and 254 nm) or UV (10-08000, emitting only at 254 nm) spectrum. The lamps were inserted into a quartz sleeve and placed in the central axes of the glass column. Different intensity of VUV irradiation was achieved from VUV/UVC that release different proportions of VUV (the full release is set at 100%). Initial solution pH was uncontrolled but measured, which remained around 6.23 during the reactions. Hence, initial solution pH was adjusted with 0.1 M HCl and NaOH solution to investigating the influences of pH. For each experiment, samples were withdrawn from the photo-reactor at predetermined time intervals and analyzed timely.

2.3. Analytical methods

The concentration of methylene blue (MB) and UV-Vis absorption spectra of aqueous was analyzed on an UV-Vis spectroscopy (Specord® 200 plus, Analytik Jena, Germany). Total organic carbon of the sample was determined using a TOC analyzer (N/C 3100, Analytik Jena, Germany). Quantitative analysis of $HCOO^-$, NO_2^-, NO_3^-, and SO_4^{2-} was conducted by Ion Chromatograph (Metrohm Eco IC, Switzerland), and NH_4^+ was measured by Salicylic acid spectrophotometry. The hydrogen peroxide generated during VUV/UV photolysis was measured by KI method (Kormann et al. 1988). Solution pH was measured with an FE28 pH meter (Mettler-Toledo, Switzerland). A LC-MS 8040 system (Shimadzu Corporation, Japan) was used for analysis of the degradation products of MB.

3. Results And Discussion

3.1 Effect of typical factors on the MB degradation

3.1.1 Effect of VUV power

The influence of VUV power on degradation of MB by VUV/UVC irradiation was investigated. As shown in Fig. 1a, the MB degradation process was conformed to the pseudo-first order reaction. The reaction kinetics constant of MB degradation increased from 0.0235 to 0.1729 min^{-1} with the VUV power

increasing from 10–100% (VUV full power was set as 100%). In the VUV/UVC system, the energy of photon from VUV irradiation at 185 nm reaches 6.7 eV, it is higher than the threshold energy for photochemical induced splitting of water (Nikogosyan &Görner 1992) and the bond dissociation energy (BDE) of MB molecular (Huang et al. 2013). More photon generated to destroy MB directly increase with the VUV power. The increasing VUV power also enhances the yield of ·OH and HO_2·, resulting in higher degradation efficiency of MB.

3.1.2 Effect of temperature

The effect of temperature on the degradation efficiency of MB was investigated, and results are shown in Fig. 1b. The MB degradation process at various temperature followed pseudo-first-order reaction kinetics, and the constants increased from 0.132 to 0.239 min^{-1} when temperature increased from 288 to 318 K. Furatian (Furatian &Mohseni 2018) reported that the 185 nm photolysis of H_2O is fairly insensitive to temperature due to the absorbance of water is negligible. In VUV/UVC irradiation system, two ·OH can merge into one H_2O_2 molecule (Eq. 3). As the previous reported, the rise of temperature results in an enhancement in the generation and reactivity of ·OH together with a decomposition of H_2O_2 (Sanz et al. 2013). Moreover, the quantum yield of ·OH and molecular diffusion higher with the sequential increase of high temperature (Cao et al. 2020). It was attributed to the radiation intensity of the ultraviolet lamp enhanced by the rise of temperature. To the light source, the optimum working temperature range of LPUV is 313 ~ 315 K (40 ~ 42 ℃) (Masschelein 2002) and the efficiency could be increased with the rise of temperature during 288 ~ 318 K. The Arrhenius plot for the MB degradation is displayed in Fig. S2. According to Arrhenius formula, the apparent activation energy of MB degradation was calculated 14.72 $kJ·mol^{-1}$. This data is similar to the degradation of MB in the UV/TiO_2 photocatalytic system (14.45 $kJ·mol^{-1}$) (Lee et al. 1999) and in the electrical discharge plasma (13.09 $kJ·mol^{-1}$) (Benetoli et al. 2011).

3.1.3 Effect of initial pH

To further explore the rule of MB decomposition in VUV/UVC irradiation system at different conditions, degradation of MB was evaluated at different initial pH values. As shown in Fig. 1c, MB was degraded entirely at various initial pH in 30 min, but initial pH has different effects on the degradation rates. When solution pH increased from 3.02 to 9.19, the pseudo-first-order reaction kinetics constant increased from 0.123 to 0.203 min^{-1}, though to a lesser extent, and then reduced to 0.181 min^{-1} as pH increased to 10.98. It should be noted that the effect of pH on MB photodecomposition was not significant except at high pH values. The improvement of MB degradation with increase of pH can be attributed to either consumption of ·OH by OH^- (Eq. 4). As initial pH increased from 3.03 ~ 9.19, few of ·OH were quenched by OH^- (Zhang et al. 2020) and leading to MB degradation. However, as pH increased to 10.98, too much ·OH quenched by OH^- and inhibited the MB degradation. For the oxidizing nature of ·OH, the oxidation potential of ·OH reduced with pH from 2.59 V (pH 0) to 2.18 V (pH 7.0), and ·OH could be further converted to $O^{\cdot-}$ (E^0 = 1.64 V) under alkaline conditions (Koppenol &Liebman 1984). In addition, the light screening effect of OH^- (ε_{185} > 3099 M^{-1} cm^{-1}) (Sauer et al. 2004) also reduced the ·OH generation (ε_{185} > 1.8 M^{-1} cm^{-1}) (Weeks et al. 1963).

$$2 \cdot OH \leftrightarrow H_2O_2$$

$k = 5.5 \times 10^9\ M^{-1}s^{-1}$ (3)

$$\bullet OH + OH^- \rightarrow H_2O + O^{\bullet -}$$

$k = 1.2 \times 10^{10}\ M^{-1}s^{-1}$ (4)

3.1.4 Effect of initial MB concentration

Figure 1d shows the degradation process of MB at the different initial concentration in VUV/UVC irradiation system. Apparently, the MB degradation rate decreased gradually with increased initial MB concentration, the pseudo-first-order reaction kinetics rate constant reduced from 0.554 to 0.058 min^{-1} when the initial MB concentrations increased from 10 to 70 mg/L. Yang et al. (Yang et al. 2020) observed the same trends in the degradation of atrazine using VUV/UVC/Fe. In the VUV/UVC system, MB achieved effective degradation at low MB concentration due to the relative abundant photons and ROS. However, as initial concentration of MB increased, MB and its products compete with photons and ROS. Furthermore, the VUV photons was absorbed by MB and its products, and inhibited the generation of ROS by the light screening effect (Li et al. 2017).

3.2 Degradation mechanism of MB in different reaction process

VUV/UVC radiation process is a complex reaction system due to the coexist of radical reaction and photochemical reaction. In addition to VUV induced ROS processes and UVC photolysis, the generation of H_2O_2 cannot be neglected. Through combination of ·OH and HO_2· species (Eqs. 4 and 5), H_2O_2 could be generated in the VUV/UVC photolysis water process. As shown in Fig. 2a, H_2O_2 concentration increased and leveled off at a *quasi*-stationary concentration of 15.15×10^{-6} M (0.52 mg/L), and the maximum concentration was 38.56×10^{-6} M (1.31 mg/L) at 5 min. H_2O_2 concentration raised continuously until to the maximum in a circular photo-reactor also reported on previous study (Moussavi et al. 2018). In this process, the H_2O_2 was formed mostly by recombination of ·OH (Zhang et al. 2020). After that, H_2O_2 was decomposed with other reactions (Eqs. 6 and 7) and UVC photolysis (Eq. 8), then secondary radical generated. Ultimately, Formation and decomposition of H_2O_2 form a dynamic equilibrium, resulting in a steady-state concentrations.

$$2HO_2 \cdot \rightarrow H_2O_2 + O_2$$

$k = 8.4 \times 10^5\ M^{-1}s^{-1}$ (5)

$$H_2O_2 + \bullet OH \rightarrow HO_2^{\bullet} + H_2O$$

$k = 3.3 \times 10^7\ M^{-1}s^{-1}$ (6)

$$e_{aq}^{-} + H_2O_2 \rightarrow \bullet OH + OH^{-}$$

$k = 1.1 \times 10^{10}\ M^{-1}s^{-1}$ (7)

$$H_2O_2 + \underset{\leftrightarrow}{\lambda = 254nm} 2 \cdot OH$$

$\Phi(H_2O_2) = 0.5$ (8)

To investigate the individual contribution of UVC photolysis, and UVC/H_2O_2 to MB degradation in VUV/UVC system, the degradation experiments were conducted individually in above three systems. As shown in Fig. 2b, direct photolysis by UVC caused slight degradation of MB, where only 6.96% of MB was removed after 30 min. By contrast, MB was degraded quickly in both VUV/UVC irradiation process and UVC/H_2O_2 process. The remove rate of MB was 100% and 96.82% for VUV/UVC and UVC/H_2O_2 process, respectively.

Sodium bicarbonate (SB) and 1, 4-benzoquinone (BQ) were respectively selected as organic quencher for ·OH and HO_2·. As shown in Fig. S3, MB removal efficiency and pseudo-first-order kinetic constant k reduced leveled off as SB and BQ concentration were 60 and 0.5 mM, respectively, suggesting that ·OH and HO_2· were the ROS in VUV/UVC irradiation process. The degradation of MB in UVC alone, VUV/UVC alone and UVC/H_2O_2 process are shown in Fig. S4. MB degradation by UVC irradiation, VUV/UVC irradiation and UVC/H_2O_2 system well followed a pseudo-first-order kinetics and the degradation rate constant were 0.002, 0.168 and 0.161 min^{-1}, respectively. As shown in Fig. S4 (a), no obvious effect on MB degradation was found in the UVC irradiation process with addition of quenchers. It was confirmed that quenchers had negligible influence on the degradation of MB in UVC process. As can be seen in Fig. S3 (b and c), degradation of MB has been inhibited in VUV/UVC irradiation and UVC/H_2O_2 process observably when SB or BQ added. It demonstrated that ·OH and HO_2· had been generated in VUV/UVC irradiation and UVC/H_2O_2 process. Additionally, it should be noted that the weak MB degradation was observed though ·OH and HO_2·has been quenched, which indicated the effect of direct photolysis on MB degradation.

The contribution of ·OH, HO_2· and UVC photolysis to degradation of MB was further evaluated with experiments performed with the ROS quenching tests. The contribution ratios of ·OH, HO_2· and UV photolysis were calculated as below equations: (Zhang et al. 2019b):

$$R_{\cdot \mathrm{OH}} = \frac{k_{MB} - k_{SB}}{k_{MB}} \quad (9)$$

$$R_{\mathrm{HO}_2\cdot} = \frac{k_{SB} - k_{BQ}}{k_{MB}} \quad (10)$$

Where $R_{\cdot OH}$ and $R_{HO2\cdot}$ represent the contribution ratios of ·OH and HO_2· in the overall MB degradation, respectively; k_{MB}, k_{SB}, and k_{BQ} are the degradation rate constants of MB with or without the presence of

SB and BQ, respectively. As shown in Fig. 2c, the contribution ratios of ·OH, HO_2·, and UVC photolysis were 90.12%, 3.85%, and 6.03% in VUV/UVC irradiation process and 50.92%, 41.83%, and 5.25% in UV/H_2O_2 process. These results suggested that ·OH played a significant role on MB degradation in VUV/UVC irradiation process. Unlike this result, Li et al. (Li et al. 2016) reported that HO_2· was the predominant ROS leading to MB degradation in VUV/UVC/Fenton process. Huang et al. (Huang et al. 2013) reported that ·OH and energetic photons were the primary ROS on MB degradation in VUV/UVC/TiO_2 process. In the UVC/H_2O_2 process, ·OH can be produced through direct dissociation of H_2O_2 under UVC irradiation. In this process, numerous H_2O_2 reacted with ·OH, and generated a great deal of HO_2·. Although the oxidizing power of HO_2· is lower than ·OH (Haji et al. 2011), its lifetime is several orders longer than that of the ·OH [26, 44], and played remarkable role on MB degradation. Therefore, it concluded that both ·OH and HO_2· were the main active specie for degradation of MB in UVC/H_2O_2 process. In VUV/UVC irradiation process, ·OH formation firstly by VUV photochemical ionization of water, and then HO_2· formatted by ·OH reacting with H_2O_2. However, the concentration of H_2O_2 was lower and resulted in a small quantity of HO_2· generation. Thus, the contribution of ·OH to the degradation of MB is expected to be much higher than that of HO_2·.

UV-Vis spectrum evolution of MB in degradation process in VUV/UVC and UVC/H_2O_2 systems have been presented in Fig. 3. A rapid decrease of the absorbance of MB was observed in VUV/UVC and UVC/H_2O_2 system (Fig. 3a and 3d). The absorbance of MB was slightly decrease as addition of SB and BQ in VUV/UVC irradiation system (Fig. 3b and 3c). In the UVC/H_2O_2, the absorbance of MB decreased significantly as addition of SB and have no evident changes with BQ addition (Fig. 3e and 3f).

The maximum absorption peak blue-shifted in various systems were shown in Fig. S5. The blue-shifted was observed in maximum absorption wavelength at 664 nm in VUV/UVC and UVC/H_2O_2 system, the same phenomenon were found in photocatalytic degradation of MB process (Mir et al. 2017). The blue-shifted intensity was followed the order: VUV/UVC > UVC/H_2O_2 > UVC/H_2O_2 + SB, and other systems could be negligible. In UVC/H_2O_2 + SB process, ·OH was quenched and blue-shifted was significantly suppressed in contrast to UVC/H_2O_2 system. Moreover, the formation of demethylate products during the MB degradation process induced blue-shift of UV-Vis spectra (Rauf et al. 2010, Sandoval et al. 2017). It indicates that ·OH was the main active species for demethylation of MB. In other words, HO_2· degraded MB by destroy the chromophores.

3.3 Products and proposal of MB degradation pathway

Since the mineralization of MB results in the formation of S and N containing intermediates, the concentration of NH_4^+, NO_2^-, NO_3^-, SO_4^{2-}, and $HCOO^-$ in the VUV/UVC irradiation system were measured (Fig. 4). NH_4^+ was produced due to the oxidation of the nitrogen-containing groups in MB molecules, but NO_2^- and NO_3^- were not generated. SO_4^{2-} was not detected at the initial stage of the reaction until 10 min. In other words, nitrogen-containing groups were oxidized easier than the sulfur-containing groups in

VUV/UVC irradiation system. Additionally, $HCOO^-$ generated and remarkably increased during MB degradation, indicating that demethylation was one of the pathways for MB degradation. In addition, TOC removal rate of MB was observed low to be only 15.64% (Fig. S6).

To clarify the degradation pathway of MB by UVU/UVC irradiation, the degradation intermediates were detected by LC-MS analysis. According to the typical total ion chromatogram (TIC) shown in Fig. S7, the abundance of the intermediates during MB degradation variable in time (Fig. 5a-5f). Six major intermedias of MB degradation were identified in VUV/UVC irradiation process ($[M + 1]^+$= 272, 290, 304; $[M]^+$= 242, 256-1, 256-2). Abundance of all the intermediates first accumulated and then their abundance decreased with prolonged irradiation time.

The degradation pathway of MB under VUV/UVC irradiation is proposed in Fig. 5g. Based on the intermediates, the two possible major photo-degradation pathways of MB are proposed. In the pathway I, the parent of MB was attacked by ·OH and formatted the demethylated intermediate $[M]^+$= **256-1** or $[M]^+$= **256-2**. Intermediates $[M]^+$= **242** formed from $[M]^+$= **256-1** or $[M]^+$= **256-2** by further demethylation, and then intermediates $[M]^+$= **272** were produced from $[M]^+$= **256-1** by oxidation. In the pathway II, parent MB were oxide and produced $[M + 1]^+$= **304**, which was further demethylated to $[M + 1]^+$= **290**.

To further elucidate the degradation pathway, DFT calculation was used and the optimized structure of the MB molecule shows in Fig. 6a. As shown in Fig. 6c, the calculating Fukui functions showed that the most prominent regions of f- are localized in N and S, which indicates that these sites are susceptible for ·OH attacks. According to the MB degradation products, ·OH tended to attack the N15 and N18, agreement with the results of theoretical calculation.

4. Conclusions

This work investigated the degradation kinetics and degradation mechanism of MB in chemical-free VUV/UVC irradiation system. VUV power and initial concentration of MB significantly affected the MB degradation rate, while there were few influences from pH and temperature. The MB degradation mechanism of VUV/UVC irradiation system was different from UVC/H_2O_2 system. In the VUV/UVC irradiation system, ·OH was the major active species for MB degradation, while ·OH and HO_2· were both the primary active species in UVC/H_2O_2 system. MB was degraded through two pathways including demethylation and oxidation. DFT study was carried out and supported the degradation pathways of ·OH attack. Therefore, VUV/UVC irradiation process is an excellent method to degrade MB without any chemicals addition.

Declarations

Author Contributions

All authors contributed to the study conception and design. Material preparation, data collection and analysis were performed by Jialiang Liang, Zhijie Liang and Weichun Gao. Yinyan Guan drafted the work or revised it critically for important intellectual content. The first draft of the manuscript was written by Cong Geng and all authors commented on previous versions of the manuscript. Zhiwei Zhao and Jiyan Liang read and approved the final manuscript.

Funding

Project supported by Natural Science Foundation of China (Grant No. 51878090) and LiaoNing Revitalization Talents Program, China (Grant No. XLYC1908034XLYC2007170).

Data availability

The datasets used and analyzed during the current study are available from the corresponding author upon reasonable request.

Ethics approval and consent to participate Not applicable.

Consent for publication Not applicable.

Competing interests The authors declare no competing interests.

References

1. Badmus KO, Irakoze N, Adeniyi OR, Petrik L (2020) Synergistic advance Fenton oxidation and hydrodynamic cavitation treatment of persistent organic dyes in textile wastewater. J Environ Chem Eng 8:103521
2. Benetoli LOD, Cadorin BM, Postiglione CD, de Souza IG, Debacher NA (2011) Effect of Temperature on Methylene Blue Decolorization in Aqueous Medium in Electrical Discharge Plasma Reactor. J Brazil Chem Soc 22:1669–1678
3. Berradi M, Hsissou R, Khudhair M, Assouag M, Cherkaoui O, El Bachiri A, El Harfi A (2019) Textile finishing dyes and their impact on aquatic environs. Heliyon 5:e02711–e02711
4. Cao T, Tie-fu X, Zhao M, Xu J, Cui C (2020) Application of vacuum-ultraviolet (VUV) for phenolic homologues removal in humic acid solution: Efficiency, pathway and DFT calculation. J Hazard Mater 384:121464
5. Chen Y, Ye J, Chen Y, Hu H, Zhang H, Ou H (2019) Degradation kinetics, mechanism and toxicology of tris(2-chloroethyl) phosphate with 185 nm vacuum ultraviolet. Chem Eng J 356:98–106
6. Chintalapati P, Mohseni M (2020) Degradation of cyanotoxin microcystin-LR in synthetic and natural waters by chemical-free UV/VUV radiation. J Hazard Mater 381:120921
7. Furatian L, Mohseni M (2018) Temperature dependence of 185 nm photochemical water treatment - The photolysis of water. J Photoch Photobio A 356:364–369

8. Geng C, Liang Z, Cui F, Zhao Z, Yuan C, Du J, Wang C (2020) Energy-saving photo-degradation of three fluoroquinolone antibiotics under VUV/UV irradiation: Kinetics, mechanism, and antibacterial activity reduction. Chem Eng J 383:123145
9. Haji S, Benstaali B, Al-Bastaki N (2011) Degradation of methyl orange by UV/H_2O_2 advanced oxidation process. Chem Eng J 168:134–139
10. Hasanpour M, Hatami M (2020) Photocatalytic performance of aerogels for organic dyes removal from wastewaters: Review study. J Mol Liq 309:113094
11. Huang H, Leung DYC, Kwong PCW, Xiong J, Zhang L (2013) Enhanced photocatalytic degradation of methylene blue under vacuum ultraviolet irradiation. Catal Today 201:189–194
12. Islam MT, Dominguez A, Turley RS, Kim H, Sultana KA, Shuvo MAI, Alvarado-Tenorio B, Montes MO, Lin Y, Gardea-Torresdey J, Noveron JC (2020) Development of photocatalytic paint based on TiO_2 and photopolymer resin for the degradation of organic pollutants in water. Sci Total Environ 704:135406
13. Kecić V, Kerkez Đ, Prica M, Lužanin O, Bečelić-Tomin M, Pilipović DT, Dalmacija B (2018) Optimization of azo printing dye removal with oak leaves-nZVI/H_2O_2 system using statistically designed experiment. J Clean Prod 202:65–80
14. Koppenol WH, Liebman JF (1984) The oxidizing nature of the hydroxyl radical. A comparison with the ferryl ion (FeO^{2+}). J Phys Chem 88:99–101
15. Kormann C, Bahnemann DW, Hoffmann MR (1988) Photocatalytic production of hydrogen peroxides and organic peroxides in aqueous suspensions of titanium dioxide, zinc oxide, and desert sand. Environ Sci Technol 22:798
16. Krichevskaya M, Klauson D, Portjanskaja E, Preis S (2011) The Cost Evaluation of Advanced Oxidation Processes in Laboratory and Pilot-Scale Experiments. Ozone-Sci Eng 33:211–223
17. Lee B, Liaw W, Lou J (1999) Photocatalytic decolorization of methylene blue in aqueous TiO_2 suspension. Environ Eng Sci 16:165–175
18. Li M, Qiang Z, Pulgarin C, Kiwi J (2016) Accelerated methylene blue (MB) degradation by Fenton reagent exposed to UV or VUV/UV light in an innovative micro photo-reactor. Appl Catal B-Environ 187:83–89
19. Li M, Wen D, Qiang Z, Kiwi J (2017) VUV/UV light inducing accelerated phenol degradation with a low electric input. Rsc Adv 7:7640–7647
20. Liang J, Geng C, Li D, Cui L, Wang X (2015) Preparation and Degradation Phenol Characterization of Ti/SnO_2-Sb-Mo Electrode Doped with Different Contents of Molybdenum. J Mater Sci Technol 31:473–478
21. Lin Y, Hsueh H, Chang C, Chu H (2016) The visible light-driven photodegradation of dimethyl sulfide on S-doped TiO_2: Characterization, kinetics, and reaction pathways. Appl Catal B-Environ 199:1–10
22. Masschelein WJ (2002) : Ultraviolet Light in Water and Wastewater Sanitation, 17. Lewis Publishers, Boca Raton, FL, USA

23. Mir IA, Singh I, Birajdar B, Rawat K (2017) A Facile Platform for Photocatalytic Reduction of Methylene Blue Dye By CdSe-TiO_2 Nanoparticles. Water Con Sci Eng 2:43–50
24. Mittal H, Alhassan SM, Ray SS (2018) Efficient organic dye removal from wastewater by magnetic carbonaceous adsorbent prepared from corn starch. J Environ Chem Eng 6:7119–7131
25. Moussavi G, Shekoohiyan S (2016) Simultaneous nitrate reduction and acetaminophen oxidation using the continuous-flow chemical-less VUV process as an integrated advanced oxidation and reduction process. J Hazard Mater 318:329–338
26. Moussavi G, Rezaei M, Pourakbar M (2018) Comparing VUV and VUV/Fe^{2+} processes for decomposition of cloxacillin antibiotic: Degradation rate and pathways, mineralization and by-product analysis. Chem Eng J 332:140–149
27. Nikogosyan DN, Görner H (1992) Photolysis of aromatic amino acids in aqueous solution by nanosecond 248 and 193 nm laser light. J Photoch Photobio B 13:219–234
28. Rauf MA, Meetani MA, Khaleel A, Ahmed A (2010) Photocatalytic degradation of Methylene Blue using a mixed catalyst and product analysis by LC/MS. Chem Eng J 157:373–378
29. Sandoval A, Hernández-Ventura C, Klimova TE (2017) Titanate nanotubes for removal of methylene blue dye by combined adsorption and photocatalysis. Fuel 198:22–30
30. Sanz J, Lombraña JI, de Luis A (2013) Temperature-assisted UV/H_2O_2 oxidation of concentrated linear alkylbenzene sulphonate (LAS) solutions. Chem Eng J 215–216:533–541
31. Sauer MC, Crowell RA, Shkrob IA (2004) Electron photodetachment from aqueous anions. 1. Quantum yields for generation of hydrated electron by 193 and 248 nm laser photoexcitation of miscellaneous inorganic anions. J Phys Chem A 108:5490–5502
32. Singh K, Arora S (2011) Removal of Synthetic Textile Dyes From Wastewaters: A Critical Review on Present Treatment Technologies. Crit Rev Env Sci Tec 41:807–878
33. Tkaczyk A, Mitrowska K, Posyniak A (2020) Synthetic organic dyes as contaminants of the aquatic environment and their implications for ecosystems: A review. Sci Total Environ 717:137222
34. Wang H, Mustafa M, Yu G, Östman M, Cheng Y, Wang Y, Tysklind M (2019) Oxidation of emerging biocides and antibiotics in wastewater by ozonation and the electro-peroxone process. Chemosphere 235:575–585
35. Weeks JL, Meaburn GMA, Gordon S (1963) Absorption Coefficients of Liquid Water and Aqueous Solutions in Far Ultraviolet. Radiat Res 19:559–
36. Wen D, Li W, Lv J, Qiang Z, Li M (2020) Methylene blue degradation by the VUV/UV/persulfate process: Effect of pH on the roles of photolysis and oxidation. J Hazard Mater 391:121855
37. Xie P, Zou Y, Jiang S, Wang J, Zhang L, Wang Z, Yue S, Feng X (2019) Degradation of imipramine by vacuum ultraviolet (VUV) system: Influencing parameters, mechanisms, and variation of acute toxicity. Chemosphere 233:282–291
38. Xu S, Niu X, Hou Z, Gao C, Lu J, Pang Y, Fang M, Lu Y, Chen Y, S JK, Li T, Xu J (2020) A multifunctional gelatine–quaternary ammonium copolymer: An efficient material for reducing dye

emission in leather tanning process by superior anionic dye adsorption. J Hazard Mater 383:121142

39. Yang L, Yao G, Huang S (2020) : Enhanced degradation of atrazine in water by VUV/UV/Fe process: Role of the in situ generated H_2O_2.Chem Eng J388
40. Zárate-Guzmán AI, González-Gutiérrez LV, Godínez LA, Medel-Reyes A, Carrasco-Marín F, Romero-Cano LA (2019) Towards understanding of heterogeneous Fenton reaction using carbon-Fe catalysts coupled to in-situ H_2O_2 electro-generation as clean technology for wastewater treatment. Chemosphere 224:698–706
41. Zhang Q, Wang L, Chen B, Chen Y, Ma J (2020) Understanding and modeling the formation and transformation of hydrogen peroxide in water irradiated by 254 nm ultraviolet (UV) and 185 nm vacuum UV (VUV): Effects of pH and oxygen. Chemosphere 244:125483
42. Zhang Y, Wang W, Lee M, Yang Z, Wu Q, Huang N, Hu H-Y (2021) : Promotive effects of vacuum-UV/UV (185/254 nm) light on elimination of recalcitrant trace organic contaminants by UV-AOPs during wastewater treatment and reclamation: A review.Sci Total Environ,151776
43. Zhang Y, Xiao Y, Zhong Y, Lim T (2019a) Comparison of amoxicillin photodegradation in the UV/H_2O_2 and UV/persulfate systems: Reaction kinetics, degradation pathways, and antibacterial activity. Chem Eng J 372:420–428
44. Zhang Z, Xie X, Yu Z, Cheng H (2019b) Influence of chemical speciation on photochemical transformation of three fluoroquinolones (FQs) in water: Kinetics, mechanism, and toxicity of photolysis products. Water Res 148:19–29
45. Zhu S, Dong B, Wu Y, Bu L, Zhou S (2019) Degradation of carbamazepine by vacuum-UV oxidation process: Kinetics modeling and energy efficiency. J Hazard Mater 368:178–185
46. Zoschke K, Bornick H, Worch E (2014) : Vacuum-UV radiation at 185 nm in water treatment-A review. Water Res 52, 131 – 45

Figures

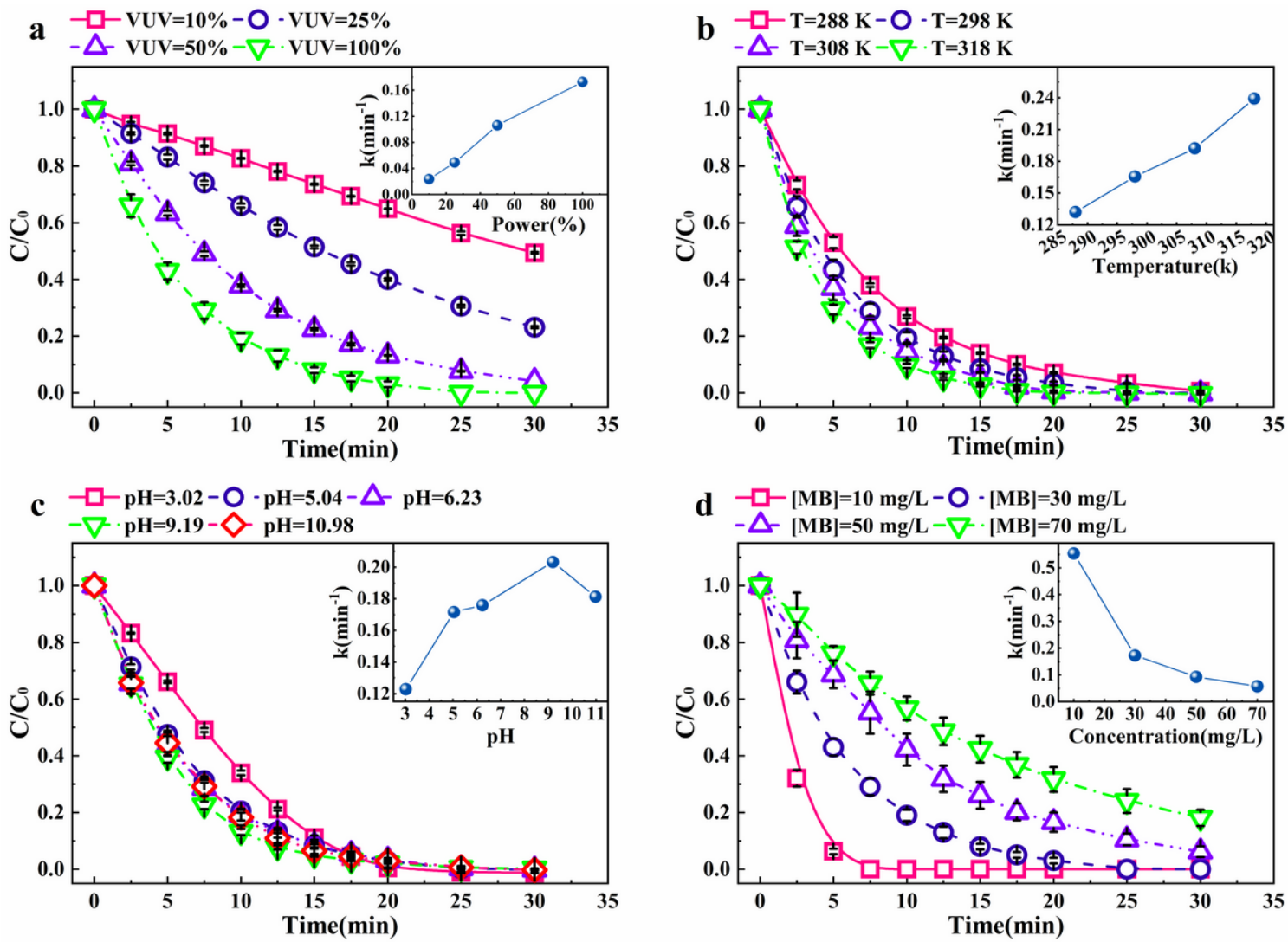

Figure 1

Degradation of MB and the rate constants (k) versus the different influence factors by VUV/UVC photolysis. (a) VUV power, (b) temperature, (c) initial pH, (d) initial concentration. Insert: Kinetic plot of MB degradation versus time. Conditions: P = 8 W, V = 300 ml, T =298 K.

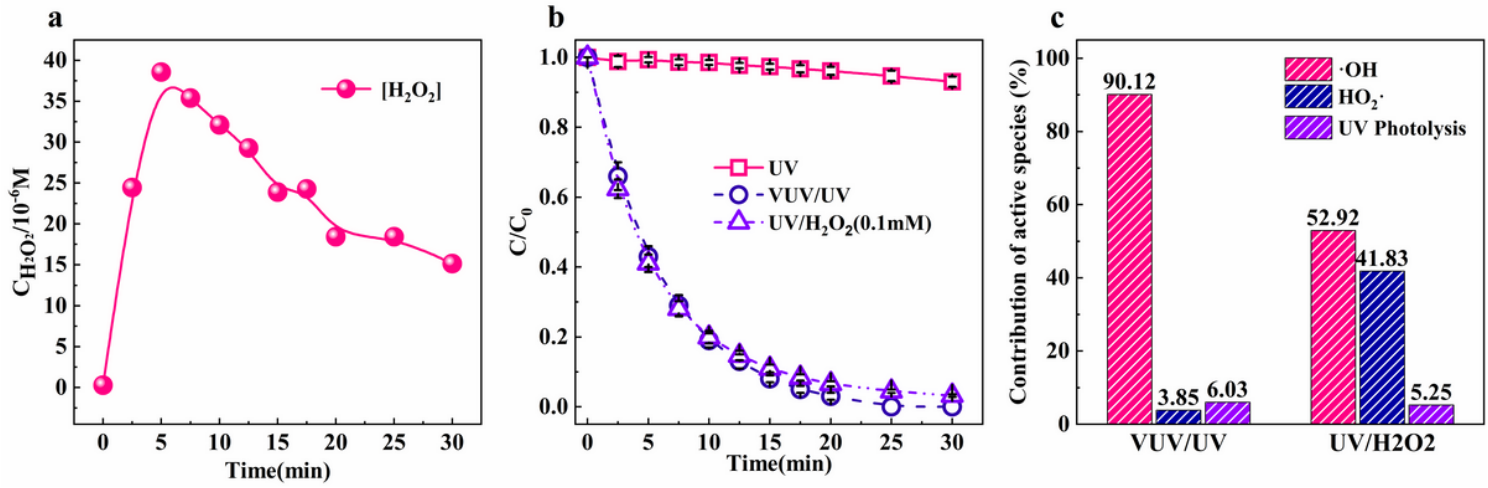

Figure 2

(a) H_2O_2 production as a function of VUV/UVC irradiation time in pure water. (b) MB degradation in different process. (c) The contribution of ·OH, HO_2· and UVC photolysis on MB degradation. Conditions: [H_2O_2] = 0.1 mM, P = 8 W, V = 300 ml, T = 298 K, [MB] = 30 mg/L.

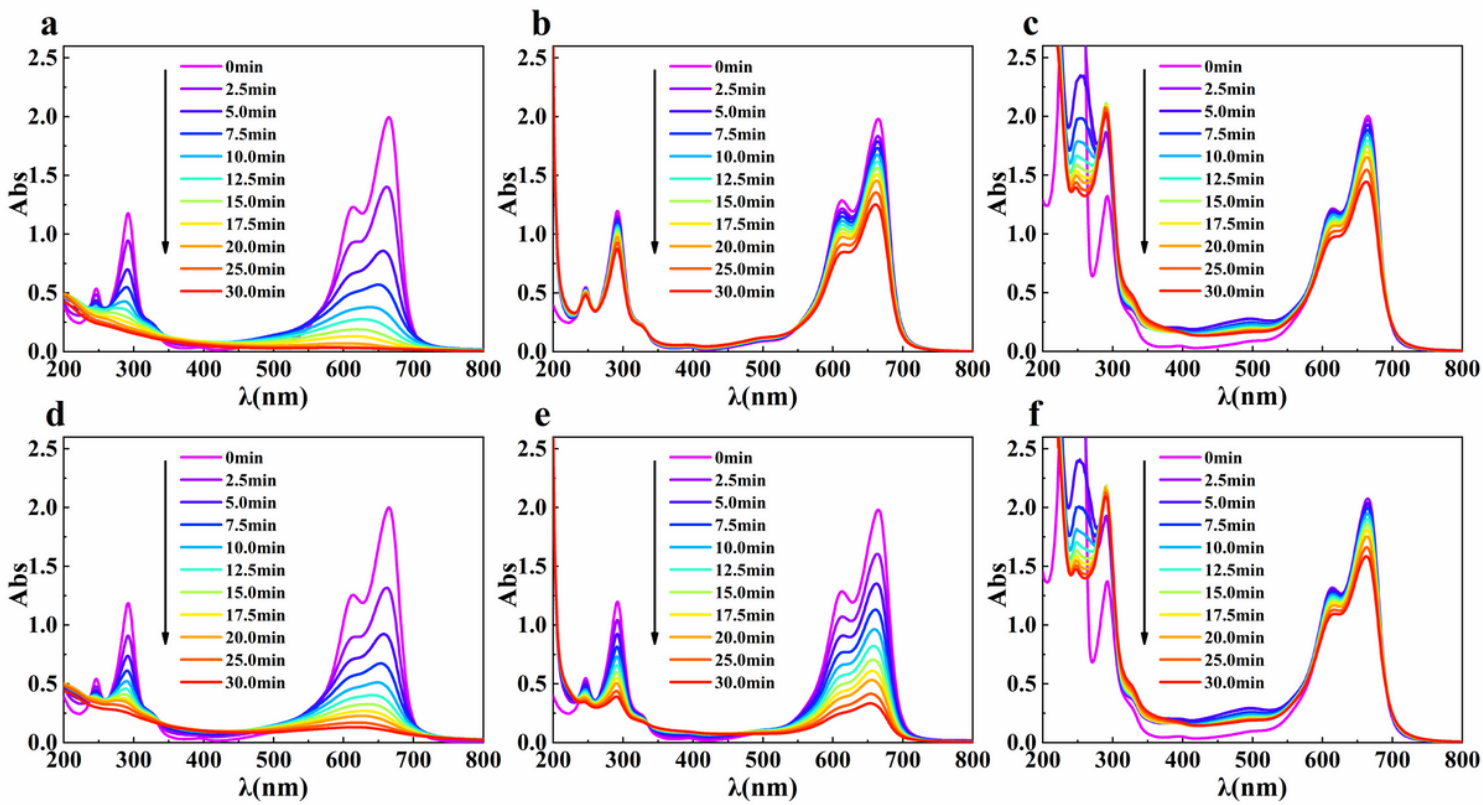

Figure 3

Time-dependent UV-Vis spectra for degradation of MB in different system. (a) VUV/UVCC, (b) VUV/UVC-SB, (c) VUV/UVC-BQ, (d) UVC/H_2O_2, (e) UVC/H_2O_2-SB, (f) UVC/H_2O_2-BQ. (Conditions: [H_2O_2] = 0.1 mM). P = 8 W, V = 300 ml, T = 298 K, [MB] = 30 mg/L, [SB] = 60 mM, [BQ] = 5 mM.

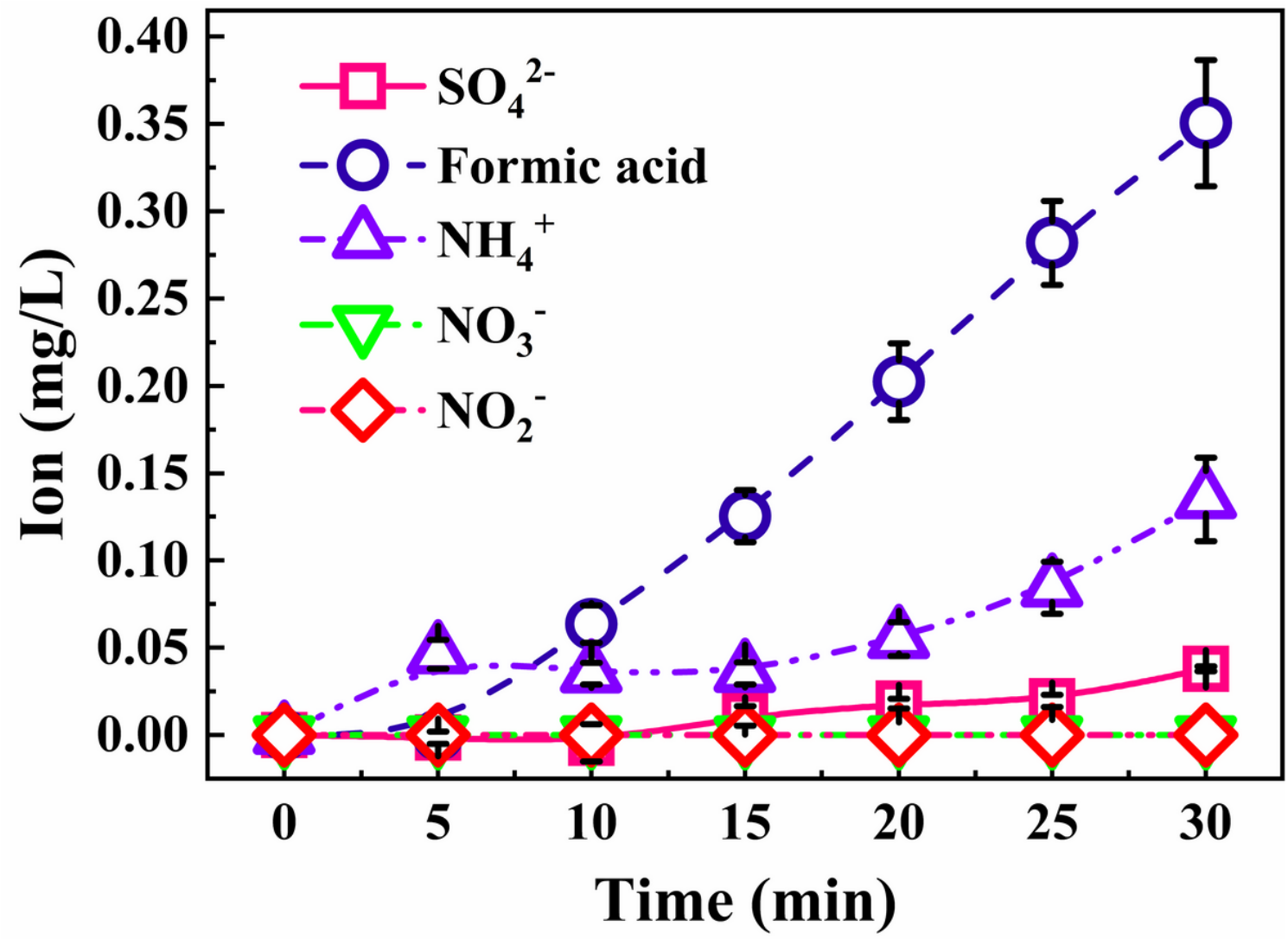

Figure 4

Formation of organic and inorganic ion products for different time. Conditions: P = 8 W, V = 300 ml, T = 298 K, [MB] = 30 mg/L.

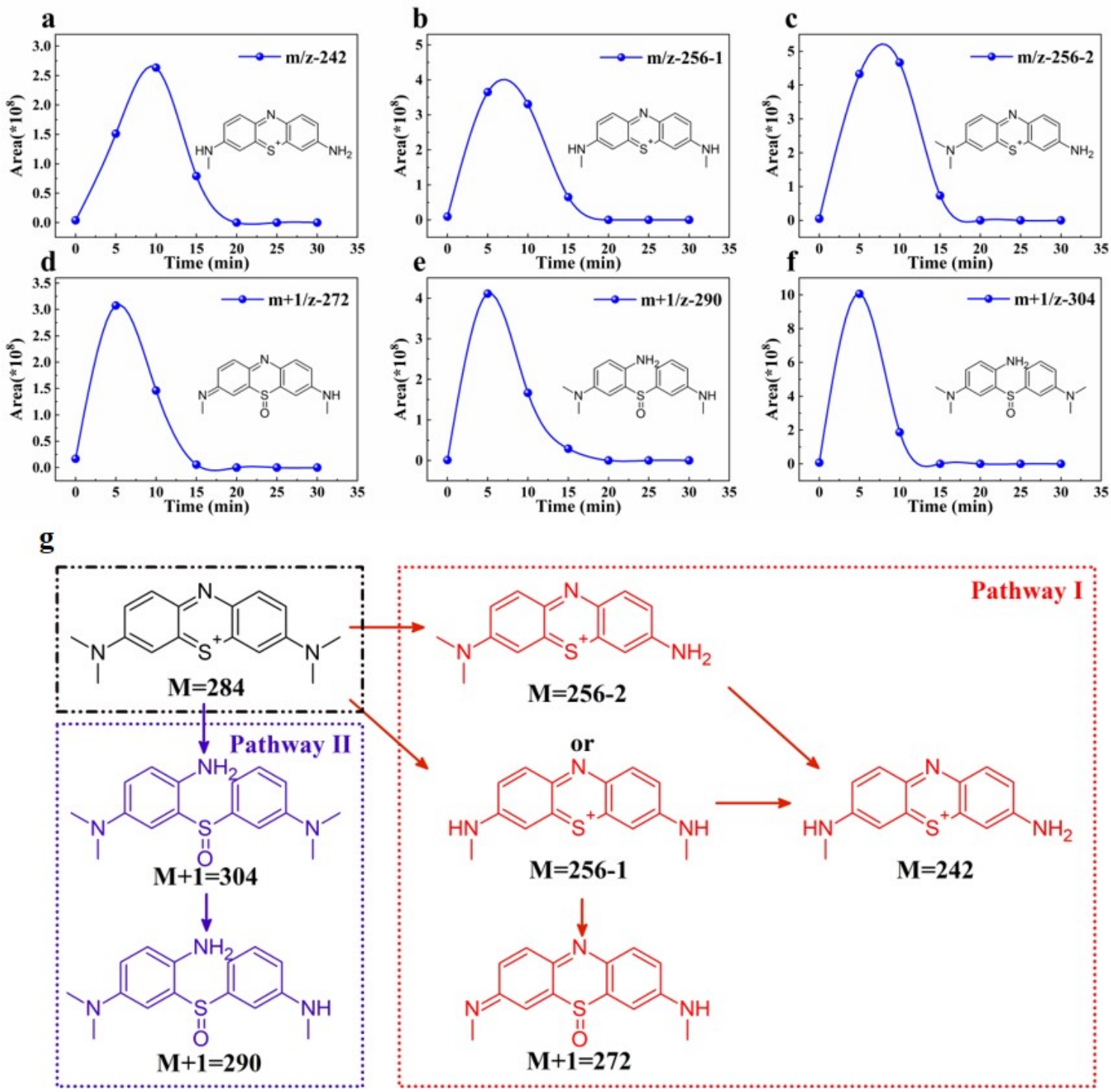

Figure 5

Evolution of MB and its degradation intermediates under VUV/UVC irradiation (a-f) and the proposed degradation pathways of MB by VUV/UVC irradiation (g).

a

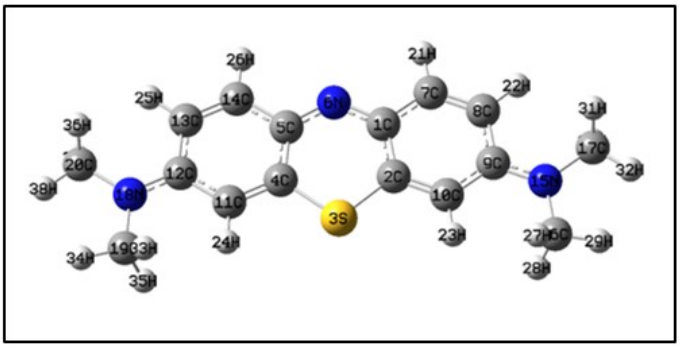

b

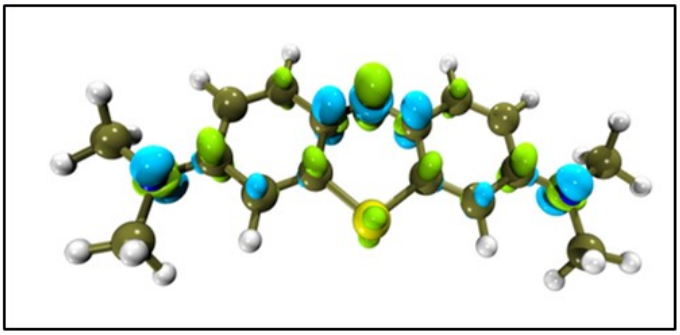

c

Atom	q(N)	q(N+1)	q(N-1)	f-	f+	CDD
1(C)	0.0437	0.0217	0.0908	0.0472	0.0219	-0.0252
2(C)	0.0055	-0.0241	0.0165	0.011	0.0296	0.0187
3(S)	0.1372	0.0354	0.1822	0.045	0.1018	0.0568
4(C)	0.0055	-0.0241	0.0165	0.011	0.0296	0.0187
5(C)	0.0437	0.0217	0.0908	0.0472	0.0219	-0.0252
6(N)	-0.1024	-0.1846	-0.0842	0.0182	0.0821	0.0639
7(C)	-0.0074	-0.0452	0.0151	0.0226	0.0378	0.0152
8(C)	-0.0393	-0.0738	0.0024	0.0417	0.0345	-0.0072
9(C)	0.0834	0.043	0.1022	0.0188	0.0404	0.0216
10(C)	-0.0671	-0.0878	-0.0298	0.0373	0.0207	-0.0166
11(C)	-0.0671	-0.0878	-0.0298	0.0373	0.0207	-0.0166
12(C)	0.0834	0.043	0.1022	0.0188	0.0404	0.0216
13(C)	-0.0393	-0.0738	0.0024	0.0417	0.0345	-0.0072
14(C)	-0.0074	-0.0452	0.0151	0.0226	0.0378	0.0152
15(N)	-0.0073	-0.0479	0.0663	0.0736	0.0406	-0.0331
16(C)	-0.0129	-0.0258	0.0049	0.0178	0.0129	-0.0049
17(C)	-0.0121	-0.0254	0.0061	0.0182	0.0133	-0.0049
18(N)	-0.0073	-0.0479	0.0663	0.0736	0.0406	-0.0331
19(C)	-0.0129	-0.0258	0.0049	0.0178	0.0129	-0.0049
20(C)	-0.0121	-0.0254	0.0061	0.0182	0.0133	-0.0049

Figure 6

DFT calculations on MB molecule: the optimized structure of the MB molecule (a); Fukui function for MB (b); NPA charge distribution and Fukui index (f – and f 0) of MB (c).

Supplementary Files

This is a list of supplementary files associated with this preprint. Click to download.

- 7Supportinginformation.docx